Supporting Information

1. Optical image of the as-fabricated micro-heater and the heater temperature and power vs. applied voltage curves; The schematic diagram of testing system for gas sensing.

2. SEM images of ZIF-8.

3. Raman spectra of the ZnO/rGO composite.

4. The XPS fitting of C 1s spectra of the ZnO/GO, and ZnO/rGO samples.

5. High resolution XPS spectra for Zn 2p, and C 1s regions of the ZnO/GO composite.

6. The XPS fitting of O 1s spectra of the ZnO/GO, and ZnO/rGO composites.

7. Current vs. Voltage behaviors of the ZnO, ZnO/GO and ZnO/rGO sensor devices.

8. Gas sensing response versus operating temperature of the ZnO and ZnO/GO sensors upon exposed to 200 ppm hydrogen.

9. The linear fitting regarding the response of the ZnO/rGO toward variable concentrations of H_2 at 400°C.

10. Response-recovery times of the ZnO/rGO to 200 ppm H_2 at different temperatures.

11. Comparison with recent studies of ZnO based H_2 sensors.

Boosting selective H_2 sensing of ZnO derived from ZIF-8 by rGO functionalization

Shiyu Zhou, [a] Jiapeng Ji,[a] Tong Qiu,[a] Liguang Wang,[a,c] Wenbin Ni,[a,c] Sheng Li,[d] Wenjun Yan,*[a,b] Min Ling*[a,c] and Chengdu Liang*[a,c]

[a] *College of Chemical and Biological Engineering, Zhejiang University, Hangzhou 310027, China*

[b] *School of Automation, Hangzhou Dianzi University, Hangzhou 310018, China*

[c] *Institute of Zhejiang University-Quzhou, 78 Jiuhua Boulevard North, Quzhou 324000, China*

[d] *Key Laboratory of Flexible Electronics (KLOFE) & Institute of Advanced Materials (IAM), Nanjing Tech University (NanjingTech), 30 South Puzhu Road, Nanjing 211800, China*

**Corresponding author:* wenjunyan@zju.edu.cn; minling@zju.edu.cn; cdliang@zju.edu.cn

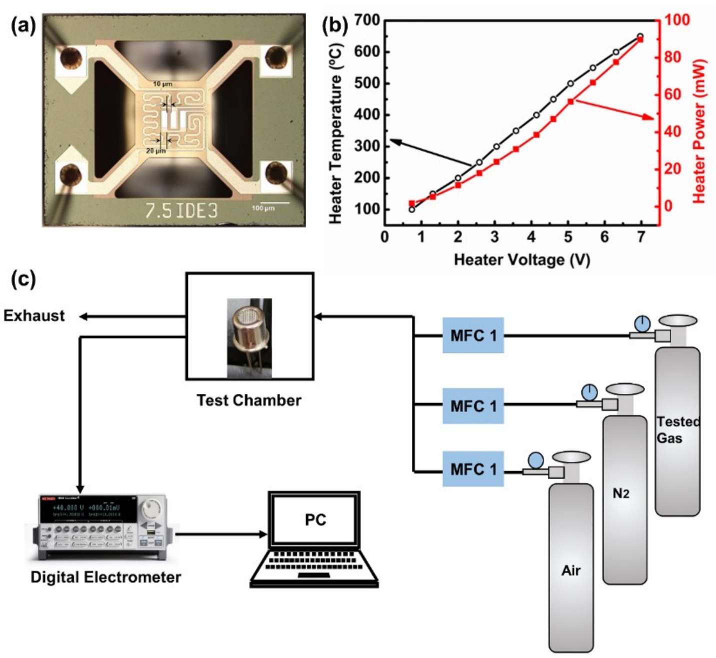

Fig. S1 (a) optical image of the as-fabricated micro-heater; (b) the heater temperature and power vs. applied voltage curves[24]; (c) The schematic diagram of testing system for gas sensing.

A pair of exposed platinum interdigital electrodes (IDEs) was fabricated on the center of the microheater to bridge the sensing material electrically. The sensing material needs to be casted on these three white stripes in the middle. The width of the platinum electrode was 20 μm, and the separation distance between the co-planar platinum electrodes was 10 µm (Fig. S1g). In order to provide necessary heating for gas sensing, the pare of IDEs were surrounded by the serpentine micro-heater. The heater temperature and power vs. applied voltage curves are shown in Fig. S1h. For example, the power consumption is nearly 39 mW for achieving a working temperature of ~ 400 °C.

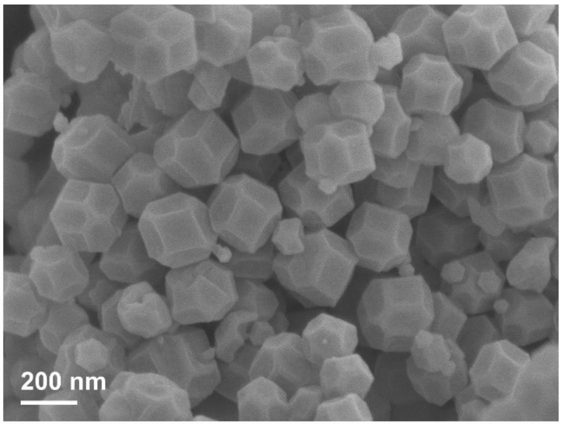

Fig. S2 SEM images of ZIF-8.

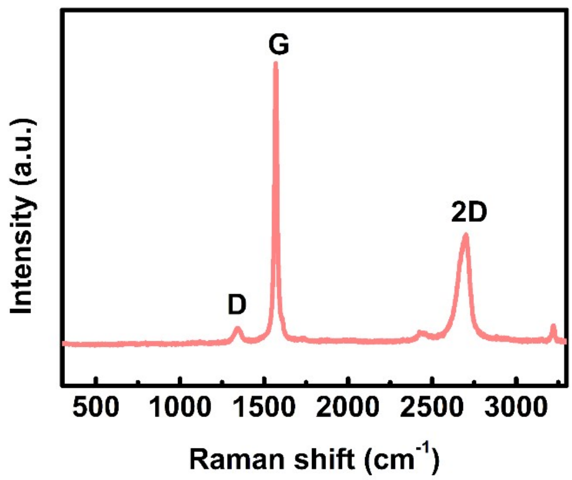

Fig. S3 Raman spectra of the ZnO/rGO sample.

Table. S1 The XPS fitting of C 1s spectra of the ZnO/GO and ZnO/rGO composites.

Sample	C-C		C-O		C=O		C(O)O	
	Binding energy (eV)	%Area	Binding energy (eV)	%Area	Binding energy (eV)	%Area	Binding energy (eV)	%Area
ZnO/rGO	284	55.84	284.9	27.52	286.0	4.13	289.1	12.52
ZnO/GO	284	46.51	284.7	35.79	285.9	14.50	288.7	3.19

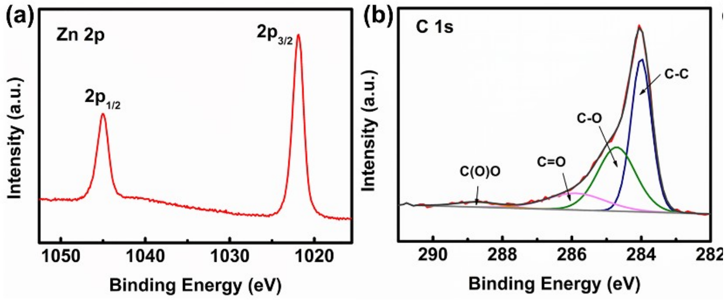

Fig. S4 High resolution XPS spectra for (a) Zn 2p and (b) C 1s regions of the ZnO/GO.

Table. S2 The XPS fitting of O 1s spectra of the ZnO/GO and ZnO/rGO composites.

Sample	O1		O2		O3	
	Binding energy (eV)	%Area	Binding energy (eV)	%Area	Binding energy (eV)	%Area
ZnO/rGO	530.5	63.37	531.9	32.99	532.8	3.64
ZnO/GO	530.6	65.27	532.0	24.01	533.3	10.71

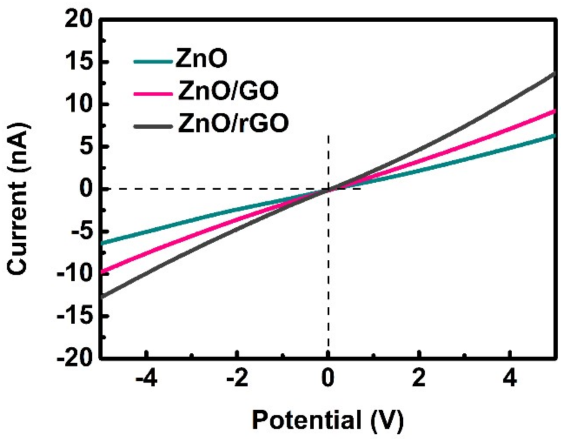

Fig. S5 Current vs. Voltage behaviors of the ZnO, ZnO/GO and ZnO/rGO sensors at room temperature.

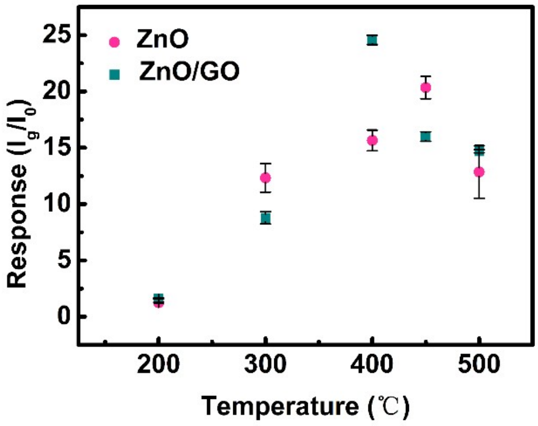

Fig. S6 Gas sensing response versus operating temperature of the ZnO and ZnO/GO sensors upon exposed to 200 ppm hydrogen.

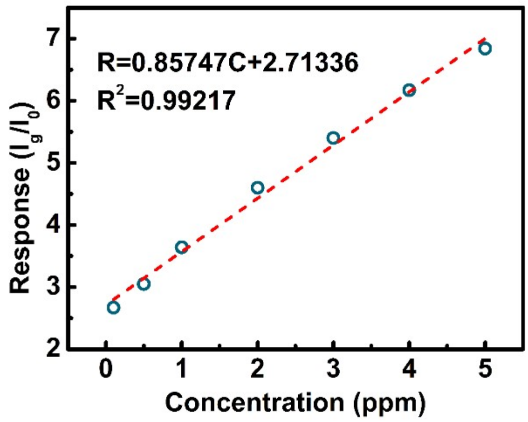

Fig. S7 The linear fitting regarding the response of the ZnO/rGO toward variable concentrations (0.1 to 5 ppm) of H_2 at 400°C.

"The limit of detection (LOD) was calculated from the sensor's signal processing performance by the common Root Mean square (RMS) method. According to the IUPAC (International Union of Pure and Applied Chemistry) definition, the signal could be considered as a true signal when the signal-to-noise ratio equals 3. Therefore, the LOD could be calculated using the following equation

$$LOD = 3\frac{N_{rms}}{slope}$$

Where Nrms is the RMS noise formula, and slope is extrapolated from the linear calibration curve as shown in Fig. S7. The limit of detection here is calculated to be 60 ppb."

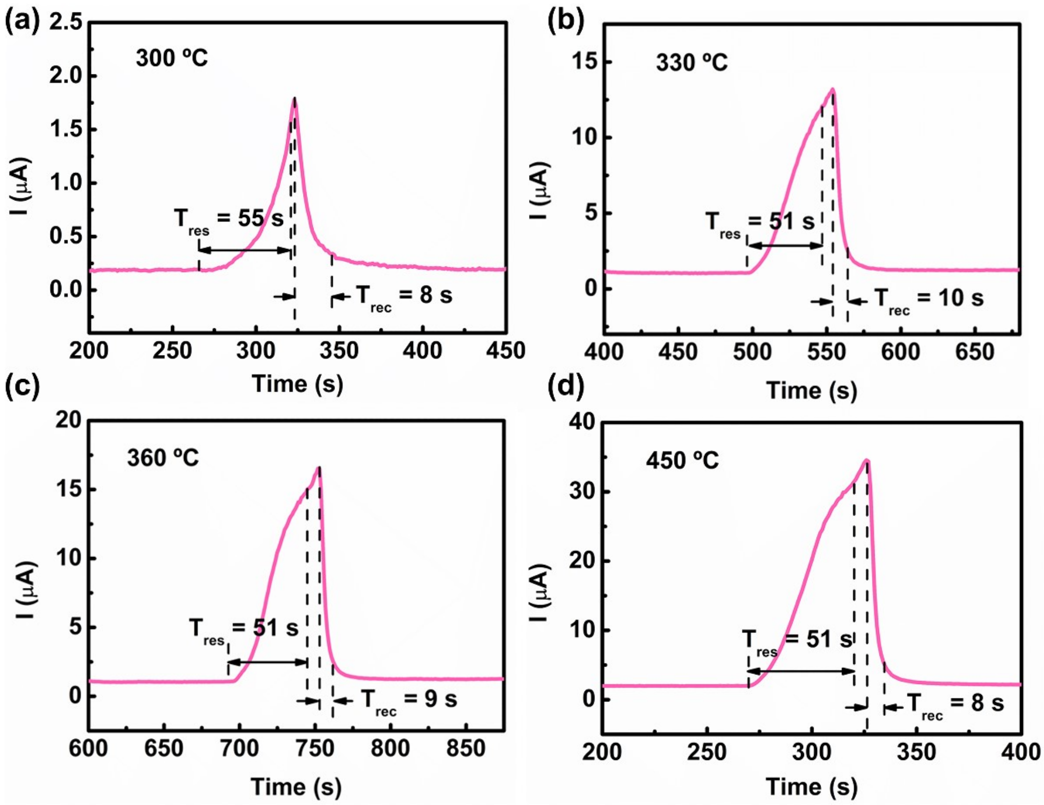

Fig. S8 Response-recovery times of the ZnO/rGO to 200 ppm hydrogen gas at different temperatures: (a) 300 °C, (b) 330 °C, (c) 360 °C and (d) 450 °C.

Table. S3 Comparison with recent studies of ZnO based H_2 sensors.

No.	Materials	LOD (ppm)	Response (R)	Ref.
1	Hierarchical ZnO inverse opal	7.5	1.21	[S1]
2	0.75 wt % rGO-4% Ni-ZnO	1	1.3	[S2]
3	Pd-decorated ZnO nanosheet	0.5	1.004	[S3]
4	ZnO nanoparticles/rGO composite	50	1.1	[S4]
5	rGO/ZnO nanocomposite	10	1.1	[S5]
6	Pd-functionalized ZnO nanowires	0.1	1.33	[S6]
7	0.2 wt% CNF/ZnO nanostructures	1	1.3	[S7]
8	ZnO/rGO composite	0.1	2.67	This work

References

S1 P. S. Hung, Y. S. Chou, B. H. Huang, I. K. Cheng, G. R. Wang, W. A. Chung, F. M. Pan and P. W. Wu, A vertically integrated ZnO-based hydrogen sensor with hierarchical bi-layered inverse opals, *Sens. Actuators, B*, 2020, **325**, 128779.

S2 V. S. Bhati, S. Ranwa, S. Rajamani, K. Kumari, R. Raliya, P. Biswas and M. Kumar, Improved Sensitivity with Low Limit of Detection of a Hydrogen Gas Sensor Based on rGO-Loaded Ni-Doped ZnO Nanostructures, *ACS Appl. Mater. Interfaces*, 2018, **10**, 11116-11124.

S3 J. H. Kim, A. Mirzaei, M. Osada, H. W. Kim and S. S. Kim, Hydrogen sensing characteristics of Pd-decorated ultrathin ZnO nanosheets, *Sens. Actuators, B*, 2021, **329**, 129222.

S4 Q. A. Drmosh, Z. H. Yamani, A. H. Hendi, M. A. Gondal, R. A. Moqbel, T. A. Saleh and M. Y. Khan, A novel approach to fabricating a ternary rGO/ZnO/Pt system for high-performance hydrogen sensor at low operating temperatures, *Appl. Surf. Sci.*, 2019, **464**, 616-626.

S5 K. Anand, O. Singh, M. P. Singh, J. Kaur and R. C. Singh, Hydrogen sensor based on graphene/ZnO nanocomposite, *Sens. Actuators, B*, 2014, **195**, 409-415.

S6 J. H. Kim, A. Mirzaei, H. W. Kim and S. S. Kim, Pd functionalization on ZnO nanowires for enhanced sensitivity and selectivity to hydrogen gas, *Sens. Actuators, B*, 2019, **297**, 126693.

S7 V. S. Bhati, A. Nathani, A. Nigam, C. S. Sharma and M. Kumar, PAN/(PAN-b-PMMA) derived nanoporous carbon nanofibers loaded on ZnO nanostructures for hydrogen detection, *Sens. Actuators, B*, 2019, **299**, 126980.